Mechanical Properties of High Nitrogen-Bearing Stainless Steel Friction Welds †

Insu WOO*, Masayoshi OZAWA**, Tutomu HORINOUCHI***, Yasushi KIKUCHI**** and Masatoshi ARITOSHI*****

Abstract

Friction welding of nitrogen-bearing stainless steels was carried out using a pressure servo-control system brake type device. The welding parameter settings comprised of rotational rate of 2400rpm, friction pressure of 70MPa for 4, 7, 10 and 15 seconds, and upset pressure of 150MPa for 6 seconds, respectively. As the friction time increased, the recrystallization zone (Region I) at the bondline vicinity increased. In contrast, increase in friction time decreased the region (Region II) where the grains were partly deformed and grown. TEM examination suggested that the intergranular phases precipitated at bondline vicinity are Cr_2N (Hexagonal, a=0.48113nm, c=0.44841nm) and CrN (Cubic, a=0.4140nm). Tensile test results indicated that nitrogen-bearing stainless steel joints have considerably higher tensile strengths than the commercial stainless steel SUS316L or SUS304 joints. However, for all welding conditions, the joint strength of high nitrogen containing-HNS-1 or HNS-2 joints showed slightly lower values than that of the base material. The inferior tensile strength of the nitrogen-bearing stainless steel joint could be due to Cr-nitrides precipitated near the bonding interface.

KEY WORDS: (High nitrogen-bearing stainless steels) (Friction welding) (Cr-nitride) (Tensile strength)

1. Introduction

Structural materials must offer the properties of nonmagnetism, high resistance to corrosion and wear, high strength and ductility according to the demands of the electronics, the precision and the cryogenic industries. Recently, as advanced materials, high nitrogen-bearing stainless steels have been introduced. Nitrogen-bearing stainless steels are known to possess good strength, hardness, toughness, corrosion resistance and non-magnetic properties[1-3].

A wider expansion in the use of these steels is, apart from other features, dependent on their joining characteristics. The ideal situation will be that joints have properties that match those of the base metal. However, this has not proved to be the case. When nitrogen-bearing stainless steels are welded using fusion welding such as MIG, TIG, electron beam, and laser welding, the completed joints have inferior strength and toughness compared to the as-received base material. This has been ascribed to the loss of nitrogen in the molten metal[4-8]. Hence, there is a need to develop joining methods with higher efficiency and which will enable joints to achieve higher strength and quality more consistently than with the fusion welding process.

Solid-state joining techniques such as friction welding do not depend on melting at the bonding interface. Therefore, friction welding offers a unique opportunity to join nitrogen-bearing stainless steels without nitrogen loss, weld porosity and weld cracking, thus producing joints with strengths approaching that of the base metal material. Friction welding has been widely applied to joining, i.e., metal to metal or metal to ceramics[9-13]. However, little attention has been paid to the application of friction welding for nitrogen-bearing stainless steels. The present work was undertaken to examine the suitability of the friction welding for nitrogen-bearing stainless steels. The microstructure and mechanical properties of friction welded joints were examined. In addition, the correlation between the friction welding phenomena and joint strength was discussed.

2. Materials and Experimental Procedures

The chemical composition of nitrogen-bearing stainless steels (HNS-1, HNS-2) and commercial stainless steels (SUS304, SUS316) used in the present study is shown in **Table 1**. The base materials HNS-1 and HNS-2 were supplied as hot extruded-bar which was heat treated at 1323K for 1 hour. The 19-mm-diameter×50-mm-long test samples were prepared for friction welding

† Received on December 18, 2000

* Post doctoral research fellow
** JAPEIC Tarasaki Center
*** Technical Assistant
**** Professor
***** Hyogo Technical Research Center

Transactions of JWRI is published by Joining and Welding Research Institute of Osaka University, Ibaraki, Osaka 567-0047, Japan.

Table 1 Chemical compositions of base materials (mass%)

Materials	N	C	Si	Mn	P	S	Cu	Ni	Cr	Mo	O	Al
HNS-1	0.272	0.011	0.19	1.50	0.019	0.0023	<0.01	9.02	22.02	<0.01	0.01	0.004
HNS-2	0.356	0.012	0.21	1.50	0.022	0.0026	0.01	9.03	22.04	<0.01	0.01	<0.002
SUS304	0.027	0.025	0.36	1.45	0.038	0.0050	-	10.2	18.15	0.27	0.001	-
SUS316L	0.034	0.026	0.29	1.28	0.037	0.0230	-	12.0	16.23	2.01	0.0078	-

experimentation with the long dimension parallel to the hot extrusion direction in the as-supplied materials. Prior to friction welding, the contacting surfaces were polished using emery paper and cleaned using acetone.

Friction welding was carried out using a pressure servo-control system brake type device. **Fig.1** shows schematically the parameters of friction welding. Among the friction welding parameters, the friction time (t_1) was particularly considered for this study. The welding parameter settings comprised of rotational rate (N) of 2400rpm, friction pressure (P_1) of 70MPa for 4, 7, 10 and 15 seconds, and upset pressure (P_2) of 150MPa for 6 seconds, respectively. The microstructural features of friction welds were examined using a combination of scanning electron microscopy (SEM) and transmission electron microscopy (TEM). SEM samples were prepared by sectioning the welded joint at right angles to the bondline. The specimens were first mechanically polished with emery paper and then etched at an aqueous 10% oxalic acid solution. Phases present at the welded joints were identified using TEM at 200kV using an energy-dispersive X-ray spectrometer (EDS) system. TEM samples were prepared as follows. Test specimens were carefully extracted by sectioning perpendicular to the weld interface and mechanically thinned to a thickness of 0.1-0.2mm. The TEM foils were then electropolished with a jet polisher using a solution of 20% perchloric acid and 80% alcohol at 273K and an electrolytic voltage 15V.

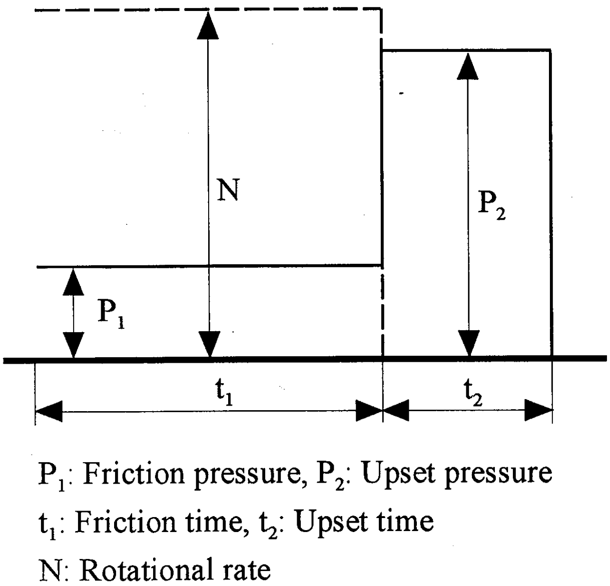

Fig.1 Schematic illustration of friction welding cycle

The mechanical characteristics of friction welds were evaluated from tensile properties measured by using a tensile test machine (REH100T type). As shown in **Fig.2**, the base materials and joints were machined to a JIS Z 2241 No.4 specimen with the parallel part of length 60mm and diameter 14mm. In addition, the bonding interface was at the center of the parallel part. A tensile test was then carried out at room temperature.

3. Results and Discussion

3.1 Base metal and joint microstructure

Fig.3 shows the optical micrographs of specimens cut perpendicular to and parallel to the extrusion direction of the HNS-2 base material. The micrographs show the elongated grain structure parallel to the extrusion direction of the HNS-2 base material and, in samples removed perpendicular to the extrusion direction, a fine mixture of about 20μm diameter polygonal grains. For the HNS-1 base material, the microstructure observed was very similar to that shown in **Fig.3**. Analysis of X-ray diffraction patterns showed that the microstructures of HNS-1 and HNS-2 base material were solely composed of γ-austenitic phases without secondary phases such as Cr-nitrides and Cr-carbides.

On the other hand, the appearance of specimen joints produced using friction pressure of 70MPa for 10 seconds and upset pressure of 150MPa for 6 seconds is shown **Fig.4**. The quantity of flash tends to decrease in the order of SUS304→SUS316L→HNS-1→HNS-2 joint. It could be also seen that the longer the friction time the greater was the quantity of flash in any of the joints considered. Among the behavior characteristics of friction welding, the burn-off has been ranked as an important factor in evaluation of joint performance. Hence, the length of burn-off in joints was measured, and a plot of this value versus the friction time is shown in **Fig.5**. The value of

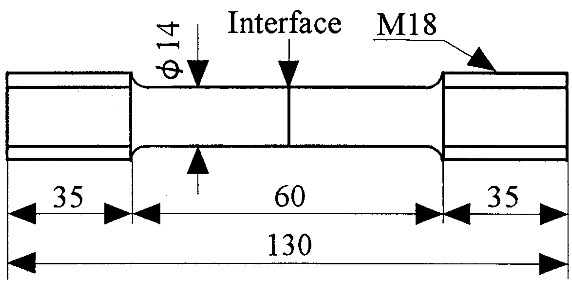

Fig.2 Shape and dimension of tensile test specimen

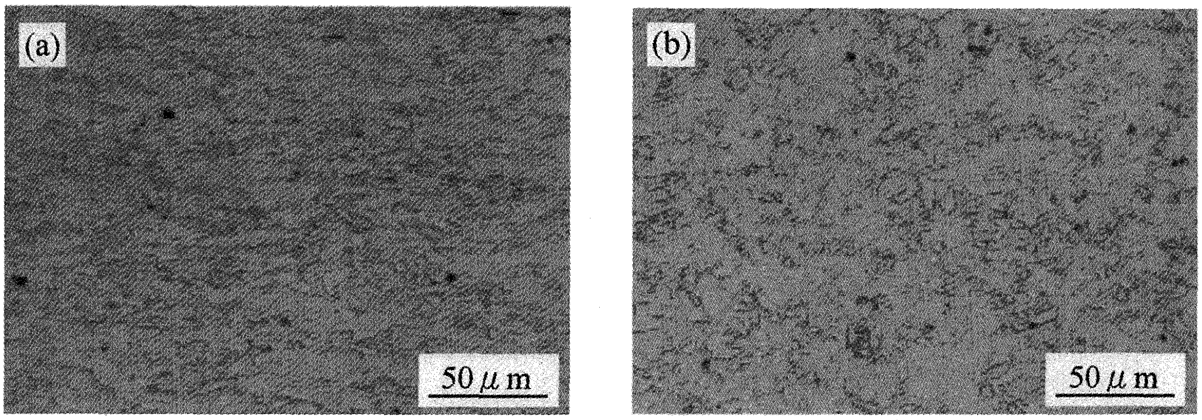

Fig.3 Optical micrographs of the HNS-2 base material: (a) Parallel to the extrusion direction
(b) Perpendicular to the extrusion direction

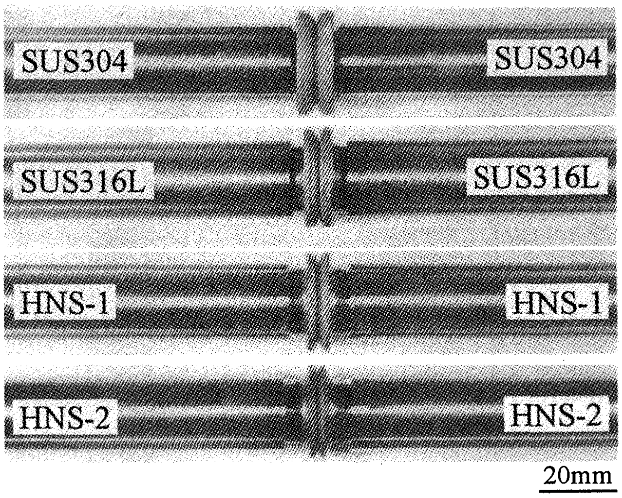

Fig.4 Appearance of specimen joints produced using friction time for 10 seconds

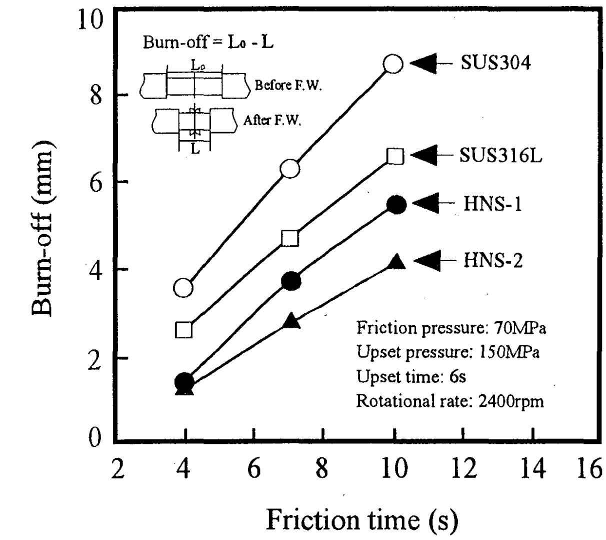

Fig.5 Effect of friction time on the burn-off in the friction welded joints

burn-off tends to increase with increasing friction time in any of the base materials considered. In addition, the burn-off of high nitrogen contained-HNS-2 joint was smaller than that of low nitrogen contained-HNS-1. This data suggests that the plastic deformation occurring in the friction welded joint increases with increasing friction time or low nitrogen containing-material.

Fig.6 shows the SEM micrograph of specimen HNS-2 joint produced using the friction time of 7 seconds. Welding defects, i.e., porosity or cracking were not observed at any of the friction welding parameters considered. For convenience, the joint microstructure is described as three distinct regions.

Region Ⅰ : the fully plasticized region on either side of the weld interface. This region contains small recrystallized-grains.

Region Ⅱ : the region where the grains are partly deformed, and grain size is larger than Region Ⅰ.

Region Ⅲ : the undeformed base material microstructure.

The average width of the Regions Ⅰ and Ⅱ from the bondline was measured for friction welds of specimen HNS-1, and a correlation between this value and the friction time is shown in **Fig.7**. As the friction time increased, the Region Ⅰ near bonding interface also increased. In contrast, as the friction time increased, the width of Region Ⅱ had a tendency to decrease. **Fig.8** shows the average width of the Regions Ⅰ and Ⅱ in HNS-1 and HNS-2 joint produced using a friction time of 7 seconds. Compared to the HNS-1 joint, for the higher nitrogen containing-HNS-2 joint, the width of Region Ⅰ was reduced and the Region Ⅱ was enlarged. During dynamic recovery, strain rate is generally considered to have an important bearing on recrystallization in the joint vicinity[12,13]. Namely, higher strain rates will accelerate

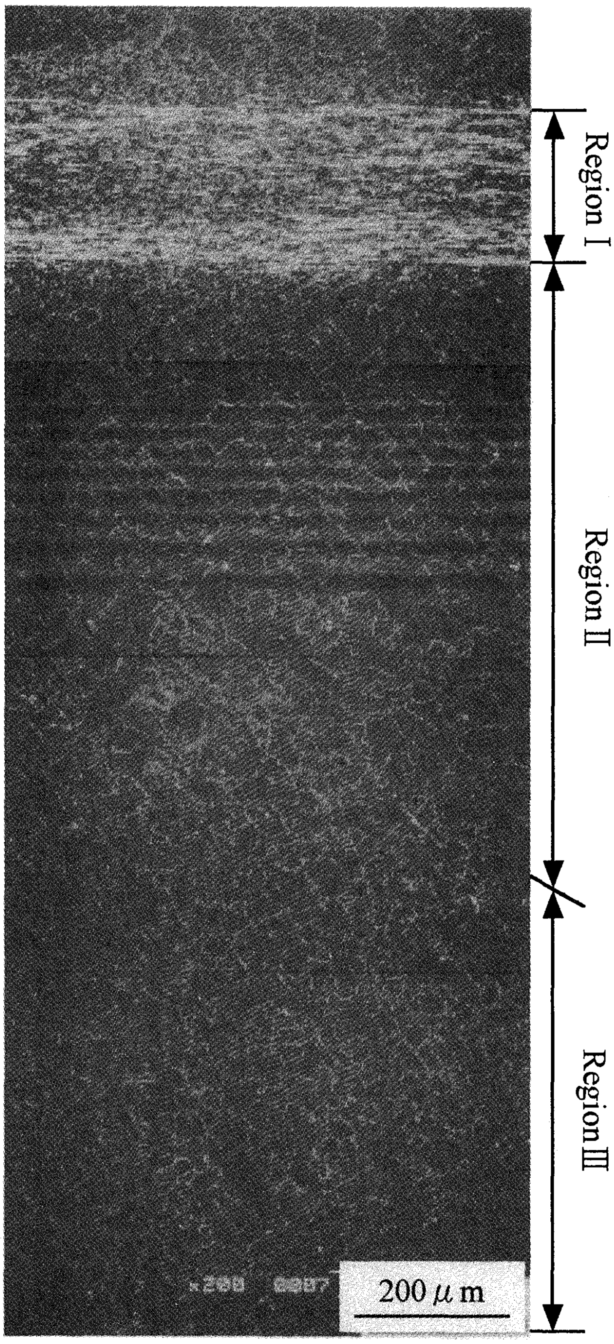

Fig.6 SEM micrograph in the HNS-2 joint produced using a friction time of 7 seconds

recrystallization during friction welding, and produce finer subgrains in the joint vicinity. The foregoing result showed that the quantity of plastic deformation in joints tends to increase with increasing friction time or low nitrogen contained-material. Therefore, the enlarged Region I was considered to be basically due to the increase in strain rate during friction welding.

On the other hand, because the periphery of the welded joint was held at higher temperature during friction welding, finer subgrains will be grown. However,

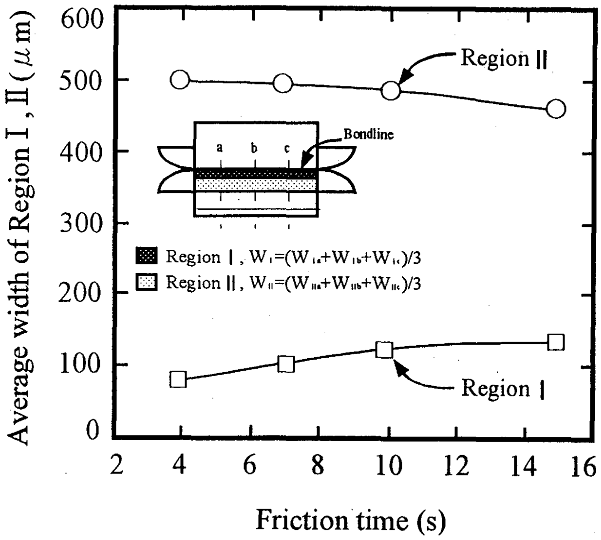

Fig.7 Effect of friction time on the average width of Region I and II in the HNS-1 joint

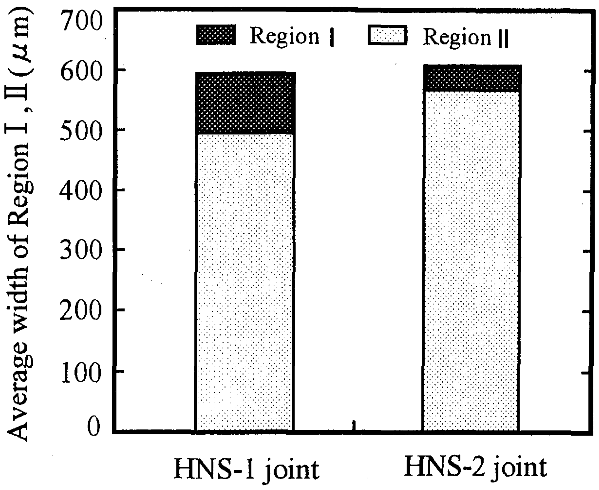

Fig.8 Average width of Region I and II in high nitrogen bearing-stainless steel joint: Friction time; 7seconds

it was noted that, regardless of friction time, the microstructure in the Region I had fine grains for the completed HNS-1 or HNS-2 joints. **Fig.9** shows a TEM micrograph of the vicinity of Region I and II in an HNS-1 joint which was friction welded using a friction pressure of 70MPa for 7 seconds and an upset pressure of 150MPa for 6 seconds. Large-shaped phases (①,③,④,⑤) and small-shaped phases (②,⑥) were apparent along the grain boundaries of Region I. However, they were not seen for the Region II. Phase identification by analysis of TEM diffraction pattern was performed to clarify the intergranular microconstituents. The electron diffraction analysis confirmed that the large-shaped phases (①,③,④,⑤) are Cr_2N(Hexagonal, a=0.48113nm,

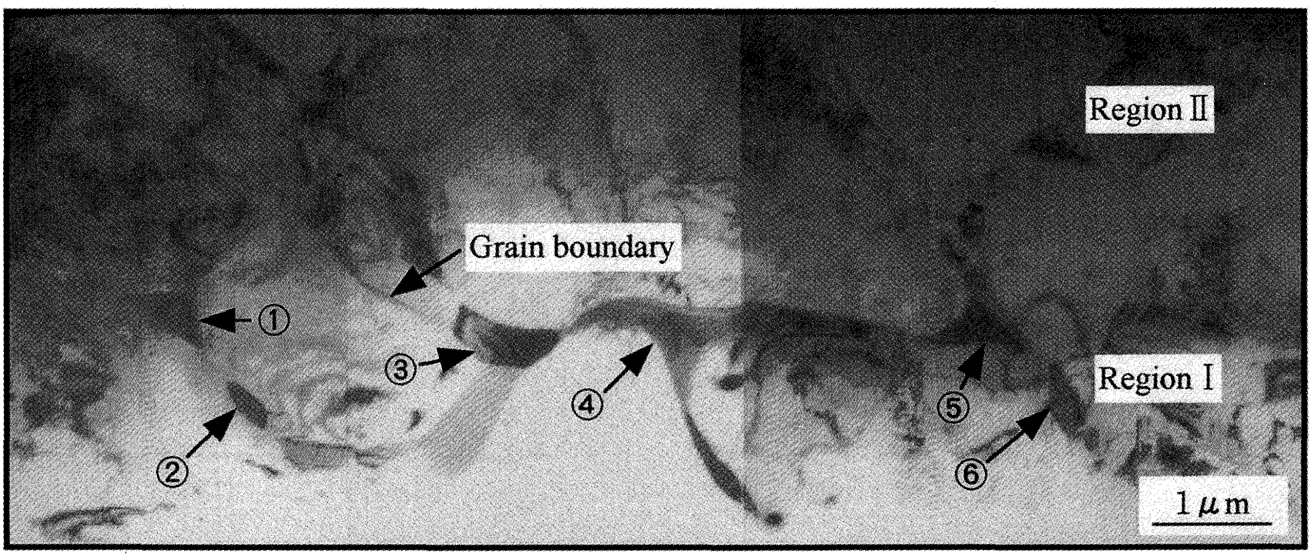

Fig.9 TEM micrograph of the vicinity of Region Ⅰ and Region Ⅱ in HNS-1 joint: friction time; 7seconds

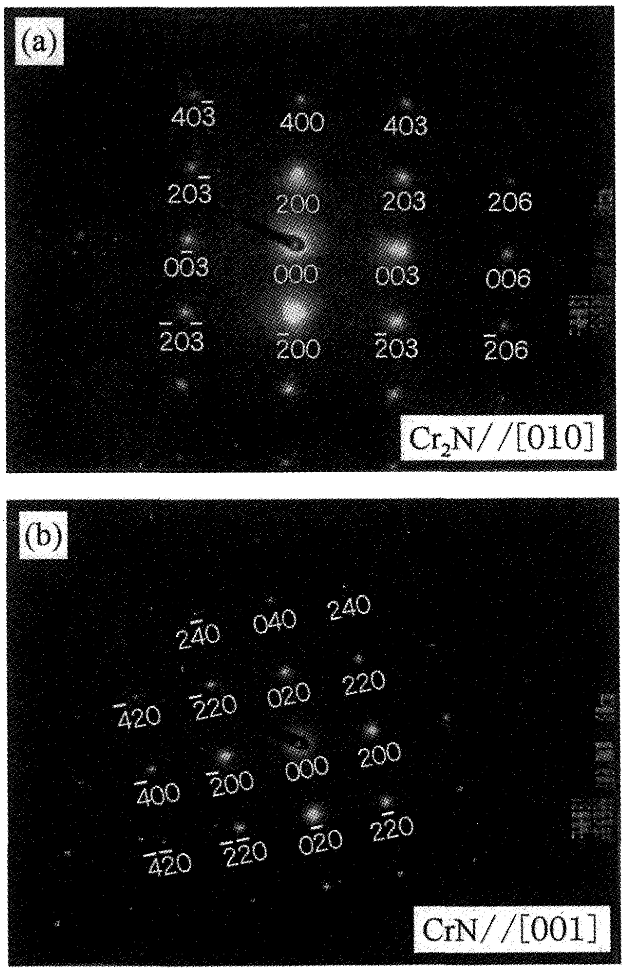

Fig.10 TEM diffraction patterns of phases in Region Ⅰ : (a) Phase①,③,④,⑤ and (b)Phase②,⑥ in Fig.9

c=0.44841nm), and the small-shaped phases (②,⑥) are CrN(Cubic, a=0.4140nm), as shown in **Fig.10**. These results suggested that the fine-grained structure of Region Ⅰ is due to a grain boundary pinning effect of the Cr-nitrides present at the grain boundaries which constitutes an obstacle to moving the recrystallized boundary during friction welding.

3.2 Mechanical property of friction welded joint

The relationship between the tensile strength and friction time of friction joints is shown in **Fig.11**. The tensile strength of base materials is also shown in **Fig.11** for comparison. A tendency was noted such that, with

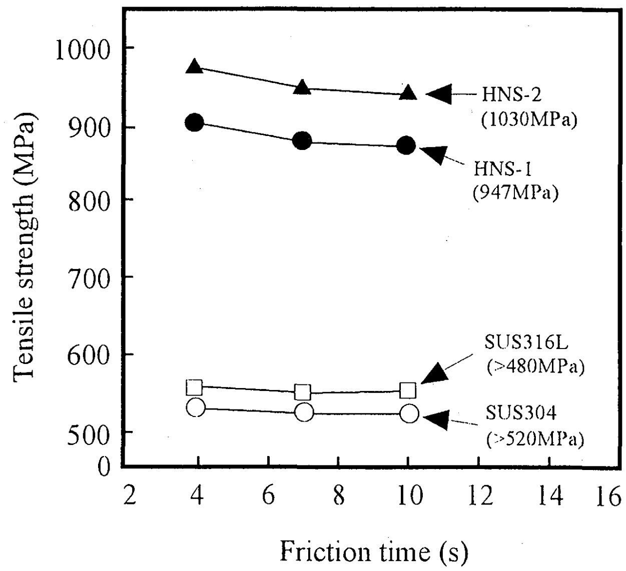

Fig.11 Effect of friction time on the tensile strength of friction welded joints(The tensile strengths of base materials are noted in parentheses)

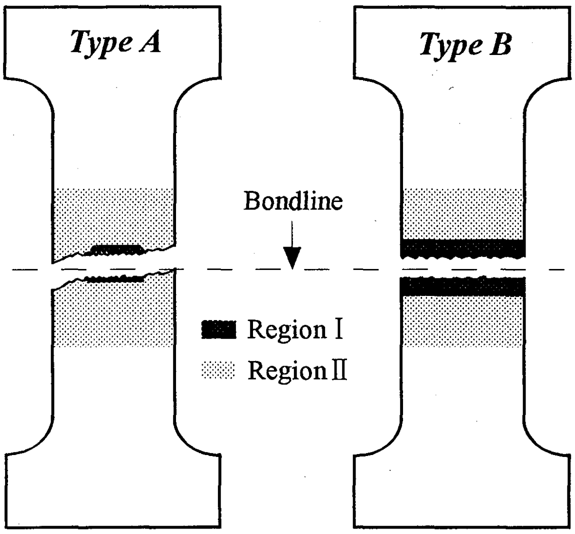

Fig.12 Failure mode in high nitrogen bearing-stainless steel joint

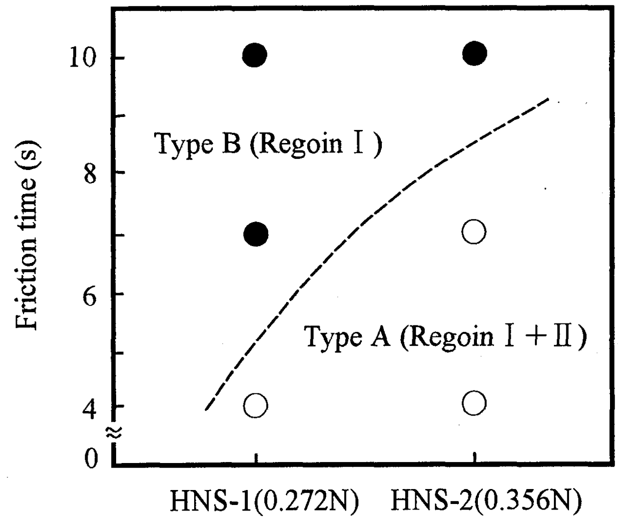

Fig.13 Effect of friction time and nitrogen content on the failure mode of friction welded joints

increasing friction time, the joint strength decreased for all specimens considered. It can also be noted that the nitrogen-bearing stainless steel joints have considerably higher tensile strengths than the commercial stainless steel SUS316L or SUS304 joint. The tensile strength of the commercial stainless steel (SUS316L, SUS30) joint was equal to or greater than that of the base material. However, for all welding conditions, high nitrogen contained-HNS-1 or HNS-2 joints showed slightly lower tensile strengths than the base material, and the joints failed near the bonding interface. Two types of failures were encountered, i.e., Region I and Region II (Type A), Region I (Type B), as illustrated in **Fig.12**. The failure mode of the joint tends to transfer from Type A to Type B with increasing friction time or low nitrogen containing-base material, as shown in **Fig.13**.

In order to clarify the influences of friction time and nitrogen content on the tensile properties of nitrogen-bearing stainless steel joints, microhardness measurements were carried out across the welded joint. **Fig.14** shows distribution of microhardness in HNS-2 joint produced using a friction time of 7 seconds. The microhardness decreased in the order of Region III → Region II → Region I. With regard to the value of microhardness each region, the Region I has a microhardness about 100Hv lower than the base material. As mentioned in the previous section, the width of Region I was enlarged with increasing friction time or low nitrogen containing-material. That is, the inferior tensile property of nitrogen-bearing stainless steel joints can be due to an increase in the width of Region I with increasing friction time or low nitrogen containing-material.

On the other hand, many researchers have suggested that intergranular Cr-nitrides diminish the mechanical and corrosion properties of nitrogen-bearing stainless steels[14-16]. As indicated above, TEM examination in the nitrogen-bearing stainless steel joint revealed the existence of Cr-nitrides precipitated at the grain boundaries of Region I. This suggests that the tensile strength of nitrogen-bearing stainless steel joints decreases, and then the bondline vicinity fails because of Cr-nitride precipitated at the recrystallized boundary of Region I. The transition from Type A to Type B with increasing friction time or low nitrogen containing-base material is considered to be attributed to an increase of Cr-nitride precipitation with increasing width of Region I. The detrimental effect of Cr-nitride on the tensile property of a friction welded joint is generally explained by a mechanism as follows. It is recognized that nitrogen is a strengthening alloy addition through its action as an interstitial solid solution strengthener. Therefore, an increase in the quantity of

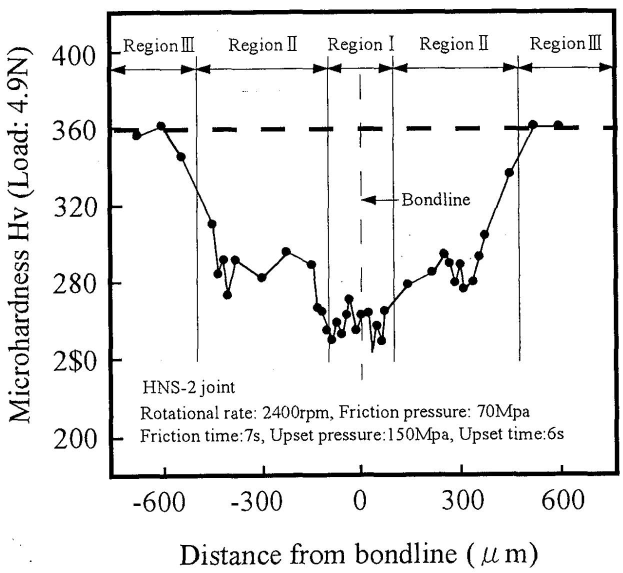

Fig.14 Distribution of microhardness in the HNS-2 joint

intergranular Cr-nitrides during friction welding reduces the nitrogen content in the matrix, which seems to be responsible for lower tensile properties of the joint due to a reduction of solid solution strengthening-effects.

4. Conclusion

This study is intended to investigate the suitability of the friction welding process for nitrogen-bearing stainless steels. The joint microstructure and mechanical property etc were examined. Based on these results, the correlation between the friction welding phenomena and joint strength was discussed. Main results obtained in this paper are as follows.

(1) The value of burn-off tends to increase with increasing friction time in any of the base materials tested. In addition, the burn-off for the high nitrogen-containing HNS-2 joint was lower than the low nitrogen-containing HNS-1 one.
(2) The welding process allowed joining of the nitrogen-bearing stainless steels, which are considered difficult to fusion weld. Welding defects, such as cracking and pores, which cause problems in fusion welding of nitrogen-bearing stainless steels, did not occur.
(3) The microstructure of nitrogen-bearing stainless steel joints is described as having three distinct regions, namely, the recrystallization zone (Region Ⅰ) near the bonding interface, the region (Region Ⅱ) where the grains were partly deformed and grown, and the undeformed base material microstructure (Region Ⅲ). As the friction time increased, the Region Ⅰ also increased. In contrast, as the friction time increased, the width of Region Ⅱ decreased.
(4) TEM examination revealed that the intergranular phases precipitated in the bondline vicinity are Cr_2N(Hexagonal, a=0.48113nm, c=0.44841nm) and CrN(Cubic, a=0.4140nm).
(5) Tensile test results showed that the tensile strength of the joints decreased with increasing friction time or low nitrogen containing-material. In addition, it can also be noted that the nitrogen-bearing stainless steel has considerably higher joint strength than the commercial stainless steel SUS316L or SUS304 joint.
(6) The reduction of tensile strength with increasing friction time and low nitrogen containing-material could be due to an increase in intergranular Cr-nitride precipitation.

References

1) H.Berns: ISIJ International, 36-7 (1996), pp.909-914
2) N.Nakamura and S.Takaki: ISIJ International, 36-7 (1996), pp.922-926
3) M.Vilpas and H.Hanninen: Materials Science Forum, 318-320 (1999), pp.603-608
4) Y.Kikuchi, F.Matsuda, T.Okabe and M.Ohta: ISIJ International, 36-7 (1996), pp.977-982
5) Y.Kikuchi, O.kamiya and H.Kobayashi: Material Science Forum, 318-320 (1999), pp.621-626
6) M.Harzenmoser, C,Rennhard, M.Hereth and M.Diener: Material Science Forum, 318-320 (1999), pp.591-596
7) Okagawa.R.K., Dixon.R.D. and Olson.D.L: Welding Journal, 62-8 (1982), pp.204s-209s
8) T.Ogawa, K.Susuki and T.Zaizen: Welding Journal, 64-7 (1984), pp.213s-223s
9) S.FUKUMOTO, H.TSUBAKINO, K.OKITA, M.ARITOSHI and T.TOMITA: Welding International, 14-2 (2000), pp.89-93
10) MIDLING and O.GRONG:Acta metall.mater., 42-5 (1994), pp.1611-1622
11) K.IKEUCHI, M.ARITOSHI, G.S.CHEN, J.BILLY and M.USHIO: Trans.JWRI, 23-1 (1994), pp.59-65
12) C.Y.Kang, T.H.North, and D.D.Perovic, Metall.Trans.A, 27A (1996), pp.4019-4029
13) K.SHINOZAKI, C.Y.KANG, Y.C.KIM, M.ARITOSHI, T.H.NORTH and Y.NAKAO: Welding Journal, 77-8 (1997), pp.289s-299s
14) J.W.SIMMONS, B.S.COVINO, Jr.,J.A.HAWK and J.S.DUNNINGH: ISIJ International, 36-7 (1996), pp.846-854
15) J.MENZEL, W.KIRSCHNER and G.STEIN: ISIJ International, 36-7 (1996), pp.893-900
16) P.J.UGGWITZER, R.MAGDOWSKI and M.O.SEIDEL: ISIJ International, 36-7 (1996), pp.901-908